Physics and implications of TeV emission from gamma-ray bursts

Susumu Inoue,[1] Lara Nava,[2,3] A. Berti,[2] Z. Bosnjak,[4] S. Covino,[2] S. Fukami,[5] F. Longo,[3,6] D. Miceli,[3,7] E. Moretti,[8] K. Noda,[5] Y. Suda,[9] I. Vovk[5,9] for the MAGIC Collaboration and multiwavelength collaborators

[1] RIKEN, Japan, [2] INAF, Italy, [3] INFN, Italy, [4] U. Zagreb, Croatia, [5] ICRR, U. Tokyo, Japan, [6] U. Trieste, Italy, [7] U. Udine, Italy, [8] IFAE, Spain, [9] MPP, Germany
E-mail: susumu.inoue@riken.jp

Abstract

Gamma-ray bursts (GRBs) are the most luminous sources of electromagnetic radiation in the Universe, of which many fundamental aspects remain poorly understood. TeV gamma rays from GRBs are expected to provide crucial new information on the physical mechanisms of energy dissipation, particle acceleration and radiation in these enigmatic objects. After decades of searches, a high significance detection of TeV gamma rays from a GRB was finally achieved for GRB 190114C with the MAGIC telescopes. This was accompanied by an extensive multi-wavelength follow-up campaign, spanning the radio band to GeV gamma rays. These observations unambiguously reveal a new emission component in the afterglow of a GRB, whose power is comparable to that of the synchrotron component. This component is satisfactorily interpreted as synchrotron-self-Compton emission with plausible afterglow parameters, and may be commonly produced in GRBs. Hadronic radiation mechanisms such as synchrotron emission by ultrahigh-energy protons are disfavored as its origin due to their low radiative efficiency. These results are a first step towards a deeper understanding of the physics of GRBs and relativistic shock waves. Further implications and prospects for the near future are briefly discussed.

Key words: gamma-ray burst: general — radiation mechanisms: non-thermal

1. Introduction

Long gamma-ray bursts (GRBs) are the most luminous sources of electromagnetic radiation known in the Universe, generated in ultra-relativistic jets during the collapse of massive stars at cosmological distances (Kumar & Zhang 2015). Prompt flashes of MeV gamma rays are followed by longer-lasting afterglow emission from radio waves to GeV gamma rays, mainly due to synchrotron radiation by high-energy electrons accelerated in external shocks in the ambient medium (Mészáros 2002; Piran 2004). Although emission of gamma rays at even higher, TeV energies by various radiation mechanisms had been theoretically predicted (Meszaros et al. 2004; Fan & Piran 2008), it had not been detected until recently, despite many years of dedicated searches (Inoue et al. 2013; Nava 2018).

A high significance detection of TeV gamma rays from a GRB was finally achieved for GRB 190114C with the MAGIC telescopes (MAGIC Collaboration 2019) (hereafter M19a). Gamma rays in the energy range 0.2–1 TeV were observed from about 1 minute after the burst, with significance exceeding 50σ in the first 20 minutes. This was accompanied by an extensive multi-wavelength (MWL) observational campaign, covering the bands from GHz up to GeV (MAGIC Collaboration et al. 2019) (hereafter M19b). Some results from these observations with emphasis on the MAGIC data appear in Noda et al. (2020) (hereafter N20). This article focuses on the MWL observations, along with the physical interpretation. For more details, see M19a and M19b.

2. MAGIC Observations

We summarize here the most salient observational results. GRB 190114C is a long GRB with measured duration $T_{90} \sim 116\,\mathrm{s}$ for Fermi/GBM and $\sim 362\,\mathrm{s}$ for Swift/BAT, at redshift $z = 0.4245 \pm 0.0005$. The isotropic-equivalent energy of the emission at ε =10–1000 keV during T_{90} observed by Fermi/GBM was $E_{iso} \sim 3 \times 10^{53}\,\mathrm{erg}$, implying that GRB 190114C was fairly energetic, but not exceptionally so compared to previous events.

Fig. 1 of M19a, N20 shows the light curve for the energy range $\varepsilon = 0.3-1\,\mathrm{TeV}$, corrected for the effects of intergalactic attenuation caused by the extragalactic background light (EBL). It is well fit with a simple power-law function $F(t) \propto t^{\beta}$ with $\beta = -1.60 \pm 0.07$. There is no clear evidence for breaks or cutoffs in the light curve, nor irregular variability beyond the monotonic decay. The

light curves in the keV and GeV bands display behaviour similar to the TeV band, with somewhat shallower decay slope for the GeV band. These properties indicate that most of the observed TeV-band emission is associated with the afterglow phase, rather than the prompt phase that typically shows irregular variability. Note that while the measured T_{90} is as long as ∼360 sec, the keV-MeV emission does not exhibit clear temporal or spectral evidence for a prompt component after $\sim T_0 + 25\,\mathrm{s}$ (Ravasio et al. 2019). The power radiated in the TeV band is comparable, within a factor of ~ 2, to that in the keV and GeV bands, during the periods when simultaneous TeV-keV or TeV-GeV data are available.

Fig. 2 of M19a, N20 presents both the observed and the intrinsic (EBL-corrected) spectra above 0.2 TeV, averaged over the time interval when the GRB is detected by MAGIC. The observed spectrum can be fit in the energy range $0.2 - 1\,\mathrm{TeV}$ with a simple power-law with photon index $\alpha_{obs} = -5.43 \pm 0.22$ (statistical error only). It is remarkable that photons are observed at $\varepsilon \sim 1\,\mathrm{TeV}$, despite the severe EBL attenuation expected at these energies (by a factor ~ 300 based on plausible EBL models). Assuming a particular EBL model, the intrinsic spectrum is well described as a power-law with $\alpha_{int} = -2.22^{+0.23}_{-0.25}$ (statistical error only), extending beyond 1 TeV at 95% confidence level with no evidence for a spectral break or cutoff. Adopting other EBL models leads to only small differences in α_{int}, compatible within the uncertainties (M19a).

Much of the observed emission up to GeV energies for GRB 190114C is likely afterglow synchrotron emission from electrons, similar to many previous GRBs (Kumar & Zhang 2015). The TeV emission observed here is also plausibly associated with the afterglow. However, it cannot be a simple spectral extension of the electron synchrotron emission. The maximum energy of the emitting electrons is determined by the balance between their energy losses, dominated by synchrotron radiation, and their acceleration. The timescale of the latter should not be much shorter than the timescale of their gyration around the magnetic field at the external shock. The energy of afterglow synchrotron photons is then limited to a maximum value, the so-called synchrotron burnoff limit of $\varepsilon_{syn,max} \sim 100(\Gamma_b/1000)$ GeV, which depends only on the bulk Lorentz factor Γ_b (Ackermann et al. 2014). The latter is unlikely to significantly exceed $\Gamma_b \sim 1000$. Fig. 3 of M19a, N20 compares the observed photon energies with expectations of $\varepsilon_{syn,max}$ under different assumptions. Although a few gamma rays with energy approaching $\varepsilon_{syn,max}$ had been previously detected from a GRB by Fermi (Ackermann et al. 2014), the evidence for a separate spectral component was not conclusive, given the uncertainties in Γ_b, electron acceleration rate, and the spatial structure of the emitting region. Here, even the lowest energy photons detected by MAGIC are significantly above $\varepsilon_{syn,max}$ and extend beyond 1 TeV at 95% confidence level. Thus, this observation provides the first unequivocal evidence for a new emission component beyond synchrotron emission in the afterglow of a GRB. Moreover, this component is energetically important, with power nearly comparable to that in the synchrotron component observed contemporaneously.

Comparing with previous MAGIC observations of GRBs, the fact that GRB 190114C was the first to be clearly detected may be due to a favorable combination of its low redshift and suitable observing conditions rather than its intrinsic properties being exceptional, although firm conclusions cannot yet be drawn with only one positive detection (M19a, N20).

3. Multi-wavelength Observations

The detection by MAGIC was announced to the astronomical community within a few hours, which triggered an extensive campaign of MWL follow-up observations involving instruments onboard six satellites and 15 ground telescopes. The frequency range covered by these observations spans more than 17 orders of magnitude, from 1 to $\sim 2 \times 10^{17}\,\mathrm{GHz}$, the most extensive to date for a GRB. The light curves of GRB 190114C at different frequencies are shown in Fig. 1 (see also M19b).

The spectral energy distributions (SEDs) in the MAGIC band are shown in Fig. 2 (see also M19b) for five time intervals, the first two for which simultaneous keV and GeV data are also available. During the first interval (68-110 s), Swift/XRT+BAT and Fermi/GBM data show that the afterglow synchrotron component is peaking in the X-ray band. At higher energies, up to ∼1 GeV, the SED decreases with energy, supported by the Fermi/LAT data. On the other hand, at even higher energies, the MAGIC data above 0.2 TeV implies a spectral hardening, independent of the adopted EBL model (M19b). This demonstrates that the newly discovered TeV radiation is not a simple extension of the known afterglow synchrotron emission, but rather a separate spectral component that was not clearly seen before.

4. Interpretation

The discovery of an energetically important emission component beyond electron synchrotron emission that may possibly be common in GRB afterglows offers important new insight into the physics of GRBs. The power-law temporal decay of the TeV emission over an extend duration suggests an intimate connection with the MWL afterglow emission. The most natural candidate is synchrotron self-Compton (SSC) radiation in the external forward shock: the same population of relativistic electrons responsible for the afterglow synchrotron emission Compton upscatters the synchrotron photons,

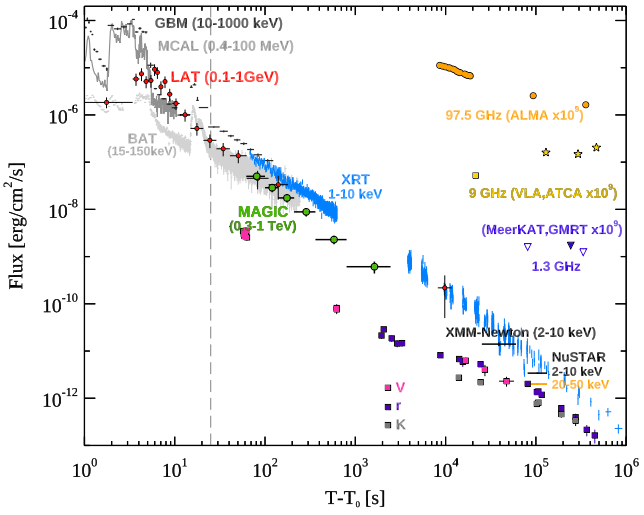

Fig. 1. MWL light curves of GRB 190114C. Energy flux at different wavelengths, from radio to gamma-rays, versus time since the Swift/BAT trigger time $T_0 = 20{:}57{:}03.19$ UT on 14 January 2019. The light curve for the energy range 0.3-1 TeV (green circles) is compared with lower frequencies. Those for VLA (yellow square), ATCA (yellow stars), ALMA (orange circles), GMRT (purple filled triangle), and MeerKAT (purple empty triangles) have been multiplied by 10^9 for clarity. The vertical dashed line marks the approximate end of the prompt emission phase. For the data points, vertical bars show the 1-σ errors on the flux, while horizontal bars represent the duration of the observation. From M19b.

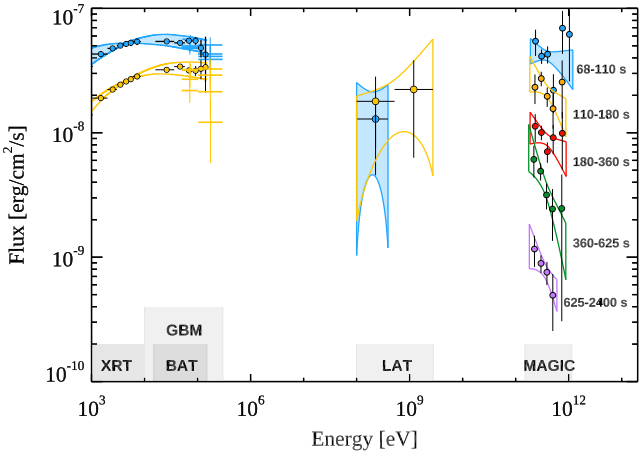

Fig. 2. Multi-wavelength spectra for time intervals t = 68-110 s (blue), 110-180 s (yellow), 180-360 s (red), 360-625 s (green), 625-2400 s (purple). MAGIC data are corrected for EBL attenuation. Also shown for the first two intervals are data from Swift/XRT, Swift/BAT, Fermi/GBM, and Fermi/LAT. For each interval, LAT contours are shown only for the energy range with detected photons. MAGIC and LAT contours correspond to the 1-σ errors of their best-fit power law functions. The Swift contours show the 90% confidence regions for the joint XRT+BAT fit with a smoothly broken power law function. From M19b.

leading to a second spectral component that peaks at higher energies (Meszaros et al. 1994; Zhang & Mészáros 2001). TeV afterglow emission can also be produced by hadronic processes such as synchrotron radiation by protons accelerated to ultra-high energies in the forward shock (Vietri 1997; Zhang & Mészáros 2001). However, due to their typically low efficiency of radiation, reproducing the luminous TeV emission as observed here by such processes would imply unrealistically large power in accelerated protons (M19a). TeV emission may also be produced via the SSC mechanism in internal shock synchrotron models of the prompt emission, but numerical modeling shows that prompt SSC radiation can account for at most $\sim 20\%$ of the observed TeV flux, and only at $t \sim< 100$ s (M19b). Henceforth, we focus on the SSC process in the afterglow. Note that afterglow SSC has also been advocated by several authors, prior to the publication of the MAGIC data (Derishev & Piran 2019; Wang et al. 2019; Fraija et al. 2019).

We model the MWL data set up to the first week after the burst as synchrotron plus SSC radiation, within the framework of the theory of afterglow emission from external forward shocks (see M19b for more details). In order to explain the relatively soft spectrum observed by MAGIC, it is favorable to invoke Klein-Nishina regime scattering for the electrons radiating at the spectral peak, as well as a moderate amount of internal $\gamma\gamma$ absorption. The energy at which the latter becomes important indicates that the bulk Lorentz factor is $\sim$140-160 at 100 s. An example of the theoretical modeling in this scenario is shown in Fig. 3 (see also M19b).

Acceptable model fits to the MWL data are found for the following physical conditions. The initial, isotropic-equivalent kinetic energy of the blastwave is $E_k >\sim 3 \times 10^{53}$ erg. The electrons swept up from the external medium are efficiently injected into the acceleration process, and carry a fraction $\epsilon_e \sim 0.05 - 0.15$ of the energy dissipated at the shock. The accelerated electrons are characterized by a non-thermal, power-law energy distribution with index $p \sim 2.4 - 2.6$, injection Lorentz factor $\gamma_m = (0.8-2) \times 10^4$ and maximum Lorentz factor $\gamma_{\rm max} \sim 10^8$ at $t \sim 100$ s. The magnetic field behind the shock conveys a fraction $\epsilon_B \sim (0.05 - 1) \times 10^{-3}$ of the shock dissipated energy. At $t \sim 100$ s, corresponding to shock radius $R \sim (8 - 20) \times 10^{16}$ cm, the density of the external medium is $n \sim 0.5 - 5\,{\rm cm}^{-3}$, and the magnetic field strength is $B \sim 0.5 - 5$ G. The latter implies that the magnetic field was efficiently amplified from values of a few μG typical of the unshocked ambient medium, due to plasma instabilities or other mechanisms (Kumar & Zhang 2015). Not surprisingly, we find that $\epsilon_e \gg \epsilon_B$, which is a necessary condition for the efficient production of SSC radiation (Zhang & Mészáros 2001).

The blastwave energy inferred from the modeling is

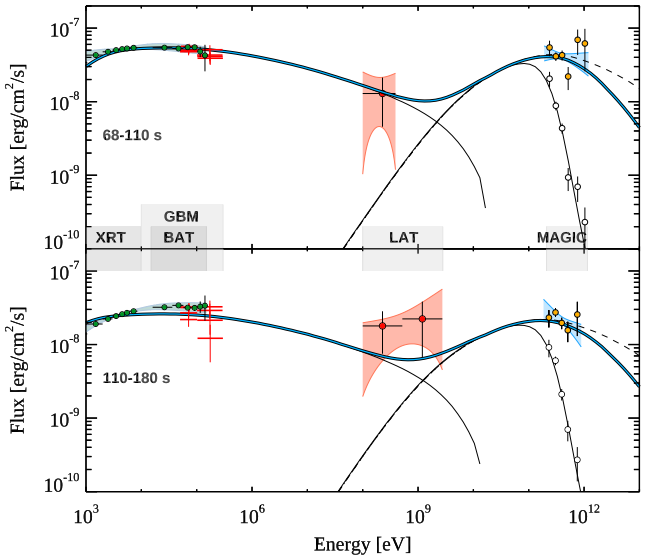

Fig. 3. Models vs MWL spectra for time intervals t = 68-110 s and 110-180 s. Thick blue: total model emission. Thin solid: model synchrotron and SSC components, including EBL attenuation. Dashed: model SSC if internal $\gamma\gamma$ opacity is neglected. The adopted parameters are: $s = 0$, $\epsilon_e = 0.07$, $\epsilon_B = 8 \times 10^{-5}$, $p = 2.6$, $n_0 = 0.5$, and $E_k = 8 \times 10^{53}$ erg (see text). Empty circles show the observed MAGIC spectrum uncorrected for EBL attenuation. See also Fig. 2. From M19b.

comparable to the amount of energy released as radiation during the prompt phase. The prompt emission mechanism must then have dissipated and radiated no more than half of the initial jet energy, leaving the other half available for the afterglow phase. The modeling also allows us to infer how the total energy is shared between the synchrotron and SSC components. We estimate that the energy in the synchrotron and SSC components are respectively $\sim 1.5 \times 10^{52}$ erg and $\sim 6.0 \times 10^{51}$ erg during t =68-110 s, and respectively $\sim 1.3 \times 10^{52}$ erg and $\sim 5.4 \times 10^{51}$ erg during t =110-180 s. Thus, earlier studies of GRBs lacking the TeV information may have been missing a significant fraction of energy emitted during the afterglow that is essential to its understanding.

The values of the afterglow parameters here fall within the typical range inferred in previous studies of GRB afterglows up to the GeV band. This indicates that SSC emission in GRBs may be a relatively common process that does not require special conditions to be produced with power similar to synchrotron radiation. Such components may then be detectable at TeV energies in other relatively energetic GRBs, as long as the redshift is low enough to avoid severe attenuation by the EBL.

These results are a first step toward a deeper understanding of the physics of GRB afterglows and related issues, such as particle acceleration and magnetic amplification in relativistic shock waves that remain poorly understood. The current situation for GRB afterglows mirrors the early 1990s for blazars when their GeV-TeV emission was first discovered, clearly revealing a new, luminous emission component beyond synchrotron emission in these objects. More afterglow detections in the very-high-energy (VHE) band should bring forth analogous advances for GRBs, including their use as probes of the EBL and intergalactic magnetic fields at high redshift. In the future, further, qualitative leaps in GRB studies may be possible through searches for VHE emission from external reverse shocks, as well as that associated with the prompt emission. Even tight upper limits on such components can provide new insight into physical conditions inside GRB jets and the origin of the prompt emission, which are some of the least understood aspects of GRBs. They can also provide powerful tests of Lorentz invariance violation.

Besides GRB 190114C, an intriguing hint was also seen in the short GRB 160821B with MAGIC, with interesting implications for future VHE follow-up of neutron star mergers triggered by gravitational waves (Inoue et al. 2017; MAGIC Collaboration 2020). The long GRB 180720B was detected with the HESS telescopes at relatively late times (∼10 hours) after the burst, also consistent with SSC afterglow emission (HESS Collaboration 2019). More recently, a GRB of the low-luminosity class, GRB 190829A, was clearly detected with HESS (de Naurois 2019). Continuing efforts with existing and upcoming gamma-ray facilities such as CTA and LHAASO promise to usher in a new era in studies of GRB physics and related topics.

References

Ackermann, M. et al. 2014, Science, 343, 42
de Naurois, M. 2019, GCN Circular 25566
Derishev, E. & Piran, T. 2019, ApJL, 880, L27
Fan, Y.-Z. & Piran, T. 2008, Front. Phys. China, 3, 306
Fraija, N. et al. 2019, ApJ, 883, 162
HESS Collaboration 2019, Nature, 575, 464
Inoue, S. et al. 2013, Astropart. Phys., 43, 252
Inoue, S. et al. 2017, 35th ICRC
Kumar, P. & Zhang, B. 2015, Phys. Rep., 561, 1
MAGIC Collaboration 2019, Nature, 575, 455
MAGIC Collaboration et al. 2019, Nature, 575, 459
MAGIC Collaboration, in preparation
Mészáros, P. 2002, ARAA, 40, 137
Mészáros, P. et al. 2004, New Astron. Rev., 48, 445
Mészáros, P. et al. 1994, ApJ, 432, 181
Nava, L. 2018, Int. J. Mod. Phys., D27, 1842003
Noda, K. et al., these proceedings
Piran, T. 2004, Rev. Mod. Phys. 76, 1143
Ravasio, M. et al. 2019, A&A, 626, A12
Vietri, M. 1997, Phys. Rev. Lett., 78, 4328
Wang, X.-Y. et al. 2019, ApJ, 884, 117
Zhang, B. & Mészáros, P. 2001, ApJ, 559, 110